

25. CV1 cells were grown in 10-cm dishes in Dulbecco's modified Eagle's medium (DMEM) with 10% fetal calf serum and transfected at 30 to 60% confluency. DNA (1 ml) was mixed with polybrene (5 μ g) [S. Kawai and M. Nishizawa, *Mol. Cell. Biol.* 4, 1172 (1984)] and was incubated with cells in 10 ml of serum-free media for 3 to 4 hours. Cells were then treated with 25% glycerol for 30 s [M. A. Lopata, D. W. Cleveland, B. Sollner-Webb, *Nucleic Acids Res.* 12, 5705 (1984)], washed, and grown in DMEM that contained insulin, transferrin, and selenium (ITS; Collaborative Research).
26. C. M. Gorman, L. F. Moffatt, B. M. Mavard, *Mol. Cell Biol.* 2, 1044 (1982).
27. We thank O. Conneely and S. Bradshaw for plasmids, and G. Caldwell and D. Scott for technical assistance. Supported by NIH grants HD-22061 and HD-07857, and the Mellon Foundation.

20 June 1990; accepted 24 September 1990

Early Enhancement of Calcium Currents by H-ras Oncoproteins Injected into *Hermissenda* Neurons

CARLOS COLLIN, ALEX G. PAPAGEORGE, DOUGLAS R. LOWY, DANIEL L. ALKON

Influx of calcium through membrane channels is an important initial step in signal transduction of growth signals. Therefore, the effects of Ras protein injection on calcium currents across the soma membrane of an identified neuron of the snail *Hermissenda* were examined. With the use of these post-mitotic cells, a voltage-sensitive, inward calcium current was increased 10 to 20 minutes after Harvey-ras oncoproteins were injected. The effects of oncogenic Harvey ras p21 protein (v-Ras) occurred quickly and were sustained, whereas the effects of proto-oncogenic ras protein (c-Ras) were transient. This relative potency is consistent with the activities of these oncoproteins in stimulating cell proliferation. Thus, this calcium channel may be a target for Ras action.

THE *ras* PROTO-ONCOGENES (*c-ras*) encode highly conserved, membrane-associated low molecular weight (21,000) proteins with guanosine triphosphatase (GTPase) activity, which serve a fundamental, but as yet poorly defined, function in the control of cell growth and development (1). Genes with point mutations encode modified proteins (an oncogenic form of Ras, v-Ras) with impaired GTPase activity, which inhibits their normal shut-off mechanism and causes sustained activation of unknown Ras targets, which probably leads to oncogenic transformation. Intracellular injection of c-Ras or v-Ras into certain quiescent cell lines induces pinocytosis and membrane ruffling (2) and, eventually, cell growth or transformation (3). The earliest reported effect after injection of Ras is an increase in pH within 10 min of injection with v-Ras but not c-Ras. This effect was attributed to a stimulation of the Na^+/H^+ antiporter (4). Activation of phosphoinositide metabolism is also induced rapidly after injection of Ras (1), but this effect occurs with other oncogenes as well (5). Ras proteins are also involved in cellular

growth induced by platelet-derived growth factor (PDGF) or epithelial growth factor (EGF) (6). Activation of EGF receptors induces early intracellular events similar to those induced by Ras injection: stimulation of phospholipid metabolism and an increase in intracellular pH, as well as transient increases in intracellular Ca^{2+} concentration (7). In fact, Ca^{2+} -free extracellular medium inhibited Ras-mediated pinocytosis and membrane ruffling in NIH 3T3 cells (2), suggesting that Ca^{2+} influx through membrane channels may be a crucial initial step in

Ras transduction of growth signals. Ca^{2+} and Na^+ (8) channels are down-regulated in cell lines transformed by Ras. Because proto-oncogenes, including *ras*, are also expressed in nervous tissue and they have been suggested to have a role in neural signaling and modification (9–11), we studied the effects of injections of Ras on voltage-sensitive inward Ca^{2+} currents in a fully differentiated, quiescent neuron from *Hermissenda*.

Under two-electrode voltage clamp of the giant left pedal 1 neuron LP_1 (150 to 200 μm diameter), we isolated a sustained voltage-dependent inward current carried by Ca^{2+} . This Ca^{2+} current was maximally activated by positive steps to 10 mV, from a holding potential of -60 mV, but it could also be activated by less positive commands (for example, to -40 mV) from more negative holding potentials (for example, -100 mV). Such characteristics are similar to those of *Aplysia* neurons (12). The Ca^{2+} current inactivated with a very long time constant (>500 ms) and was blocked by external application of cadmium or nifedipine, ruling out the possibility that it was due to a covert K^+ outward current or other inward current. Typical recordings are shown in Fig. 1. For our experiments, the inward current was elicited by depolarizing steps to 0 mV before and after iontophoretic injections of v-Ras and c-Ras, with 10 mM Ba^{2+} as the charge carrier. By pressure-injecting different concentrations of Ras into LP_1 (2 bar, 0.1 Hz, 50-ms pulses), we determined that the minimum concentration required to detect any effect on the Ca^{2+} currents was 150 $\mu\text{g}/\text{ml}$ and 300 $\mu\text{g}/\text{ml}$ for v-Ras and c-Ras, respectively. Because an increased leakage conductance and a rundown in Ca^{2+} conductance of more than 20% was observed 20 min after pressure-injection, iontophoresis with negative current pulses (-10 nA, 10 min) was sub-

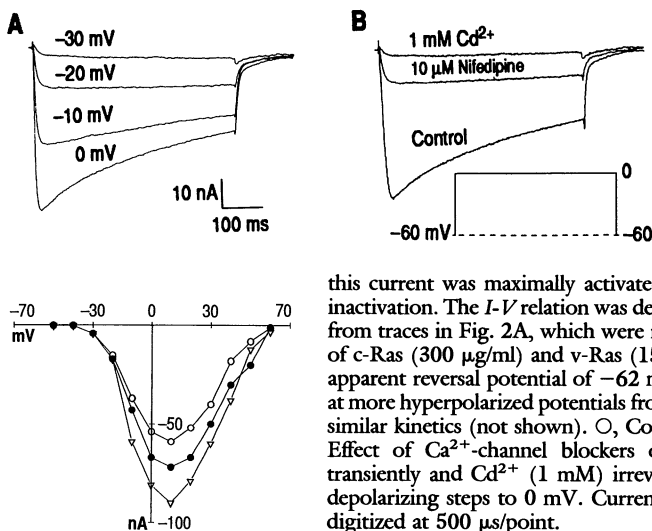


Fig. 1. Typical voltage-clamp recordings (22) of voltage-sensitive inward Ca^{2+} currents (I_{Ca}) from *Hermissenda* LP_1 neurons. Ba^{2+} (10 mM) substituted for Ca^{2+} , and there was 3 M CsCl_2 in the microelectrodes. (A) Current-voltage (I - V) relation from a -60 mV holding potential (V_{H});

this current was maximally activated at 10 mV and showed little inactivation. The I - V relation was derived from the traces above and from traces in Fig. 2A, which were recorded 30 min after injection of c-Ras (300 $\mu\text{g}/\text{ml}$) and v-Ras (150 $\mu\text{g}/\text{ml}$). The current had an apparent reversal potential of -62 mV and could also be activated at more hyperpolarized potentials from a V_{H} of -100 mV with very similar kinetics (not shown). \circ , Control; \bullet , c-Ras; ∇ , v-Ras. (B) Effect of Ca^{2+} -channel blockers on I_{Ca} . Nifedipine (10 μM) transiently and Cd^{2+} (1 mM) irreversibly reduced I_{Ca} elicited by depolarizing steps to 0 mV. Current transients in this figure were digitized at 500 $\mu\text{s}/\text{point}$.

C. Collin and D. L. Alkon, Laboratory of Molecular and Cellular Neurobiology, Section on Neural Systems, NINDS-NIH, National Institute of Neurological Diseases and Stroke, National Institutes of Health, Bethesda, MD 20892.

A. G. Papageorge and D. R. Lowy, Laboratory of Cellular Oncology, National Cancer Institute, National Institutes of Health, Fredrick, MD 20892.

sequently used to inject Ras into the neuron.

Twenty minutes after v-Ras ($n = 5$) and 30 min after c-Ras ($n = 5$) injections (Fig. 2A), Ca^{2+} current amplitudes began to increase progressively from baseline (mean \pm SD) to $60.5 \pm 7\%$ for v-Ras and to $31.6 \pm 5\%$ for c-Ras (Fig. 2B). Control injections with buffer alone or a combination of 300 $\mu\text{g/ml}$ heat-inactivated c-Ras and v-Ras ($n = 7$) had no effects (Fig. 2A). Ca^{2+} current amplitudes returned spontaneously to baseline within 40 min after c-Ras injection, but remained increased at 40 min after v-Ras injections.

To examine the temporal relation between Ca^{2+} current increases and previously shown K^+ -current reductions after Ras injections (10, 11), $LP_1 K^+$ currents were also evaluated. The early, rapidly activating and inactivating voltage-dependent outward K^+ current (I_A), and the later, Ca^{2+} -dependent outward K^+ current (I_{K-Ca}) were elicited with cesium-free microelectrodes and in the absence of blockers of these K^+ channels in the external medium, 4-aminopyridine (4-AP) for I_A and Ba^{2+} for I_{K-Ca} . Superimposed current traces elicited at -20 and 0 mV depolarizing steps before and after 150 $\mu\text{g/ml}$ v-Ras injections are shown in Fig. 3A. The K^+ currents were minimally activated with voltage steps to -20 mV, allowing clear observation of the inward Ca^{2+} current. Steps to 0 mV revealed the K^+ currents. The small inward current increased first after 20 min, with-

out any appreciable change in the amplitude of either K^+ current. Forty minutes after injection, I_A was reduced; 60 min after injection, I_{K-Ca} also appeared to be reduced. Even 60 min after injections, the Ca^{2+} currents remained increased in amplitude (Fig. 3B). These Ca^{2+} -current increases were comparable to those observed with Ba^{2+} substitution and in the presence of the K^+ -channel blockers.

The results reported here are consistent with the known biological activity of both forms of Ras. The lower GTPase activity of v-Ras, which may lead to sustained effects (13), could explain its faster and more prolonged action on Ca^{2+} channels. The delay before Ras affects the currents is consistent with the need for post-translational modification of Ras before it can bind to the cell membrane and become biologically active (2, 14). At least two possible mechanisms could explain the Ras effects on the Ca^{2+} current. First, as suggested for other G proteins, Ras could directly regulate Ca^{2+} channels (15). Alternatively, other molecular steps such as activation of a phospholipid pathway (1, 5) could be required prior to Ca^{2+} -channel activation. Similarly, Ras could act directly or indirectly on the K^+ channel. An indirect mechanism might involve, for example, the activation of a Ca^{2+} -sensitive enzyme [such as protein kinase C (PKC)] secondary to the Ras-induced enhancement of Ca^{2+} influx or phospholipid metabolites. Indeed, Ras can generate PKC-

dependent and PKC-independent signals (16).

To examine the involvement of PKC in the Ras-mediated regulation of ion channels, we treated LP_1 cells with 10 μM staurosporine, a PKC inhibitor (17). Since in dorsal root sympathetic ganglion cells, treatment with 50 μM H7 or 100 μM sphingosine causes a marked reduction of the Ca^{2+} current, we did not use these agents. Staurosporine had no detectable effect on v-Ras-induced Ca^{2+} -current increases, suggesting that the effect on Ca^{2+} channels is not mediated by PKC (Fig. 3C). By contrast, the v-Ras-induced reduction of K^+ current was inhibited by staurosporine

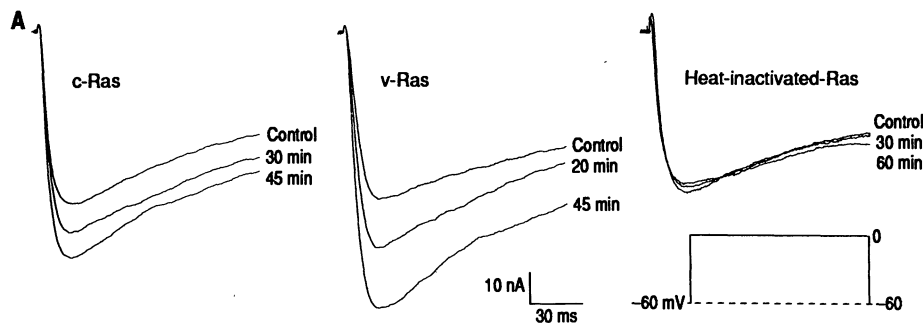


Fig. 2. Effects of c-Ras, v-Ras, and control injections on inward I_{Ca} carried by Ba^{2+} . (A) Progressive increases in current amplitude after iontophoresis with an electrode filled with c-Ras (300 $\mu\text{g/ml}$) or v-Ras (150 $\mu\text{g/ml}$). From an initial peak amplitude of 50.2 ± 3 nA ($n = 17$), the currents increased to 61.4 ± 5.9 nA ($n = 5$) 30 min after c-Ras injection and to 80.5 ± 5.1 nA ($n = 5$) 60 min after v-Ras injection. A heat-inactivated (90°C for 60 min) mix of 300 $\mu\text{g/ml}$ c-Ras and v-Ras, or buffer alone (not shown), was without effect after 60 min ($n = 7$). Run-down of I_{Ca} was minimized to less than 7% by 60 min under this recording condition, but reached more than 30% for longer time periods. The I - V relation was unchanged as was the leak conductance (measured with 20-ms opposite polarity steps) after injections. (B) Time course of Ras-mediated I_{Ca} increase. Data points are mean percent amplitude change \pm SD of I_{Ca} after v-Ras ($n = 5$), c-Ras ($n = 5$), and heat-inactivated c-Ras and v-Ras microinjections ($n = 7$) at 10-min intervals. Two-tailed t tests between control and experimental points at 20 min for v-Ras and 30 min for c-Ras were performed. ○, Control; ●, c-Ras; ▽, v-Ras; *, $P < 0.01$.

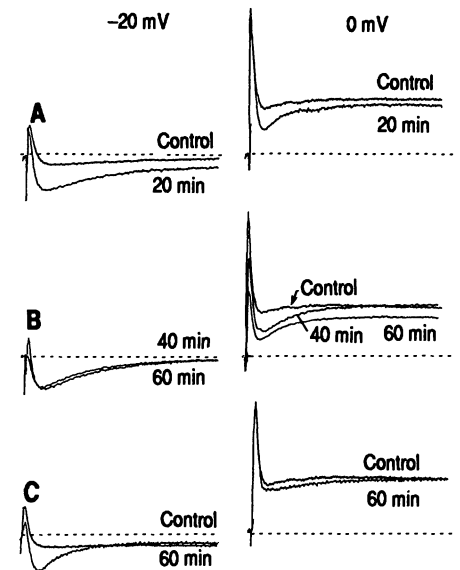


Fig. 3. Effect of Ras on K^+ currents. (A) The two superimposed current traces were elicited before (control) and after a v-Ras (150 $\mu\text{g/ml}$) injection, at the labeled time intervals with 500-ms depolarizing steps from -60 to -20 mV (left column) and from -60 to 0 mV (right column). Artificial sea water contained 10 mM Ca^{2+} and 100 mM TEA. Current was digitized at 500 $\mu\text{s/point}$. Left, I_{Ca} was elicited with depolarizing steps to -20 mV, where submaximal activation of I_{Ca} is not masked by activation of outward current and was again markedly increased at 20 min after v-Ras injections [all values are mean (nA) \pm SD]: control, 5.9 ± 3.2 ; after 20 min, 16 ± 3 , $n = 4$. Right, a voltage-sensitive, rapidly activating and inactivating outward current, peaking at 10 to 20 ms, and blocked by 4-AP (I_A) and a later, sustained outward current blocked by internal CS^{2+} measured at 250 ms (I_{Ca-K}) were not changed after 20 min. The small decrease in I_{Ca-K} at 20 min was not significant and was probably caused by an increase in inward current. (B) I_{Ca} remained elevated 60 min after v-Ras (150 $\mu\text{g/ml}$) injection (left); I_A but not I_{Ca-K} began to decrease at 40 min (right): control I_A 76 ± 5 ; at 40 min, 44 ± 4 . Sixty minutes later, I_{Ca-K} was also reduced: control I_{Ca-K} 25 ± 2 ; at 60 min, 18 ± 3 . (C) Effect of pretreatment with 10 μM staurosporine (prepared in dimethylsulfoxide) on the v-Ras-induced increase in I_{Ca} and K^+ currents. Data are from 60 min after a 150 $\mu\text{g/ml}$ v-Ras injection ($n = 7$).

treatment. Thus Ras may be acting on K⁺ channels via PKC activation. The PKC-independent nature of Ras-induced enhancement of Ca²⁺ conductance is consistent with a PKC-independent pathway for cell growth signal transduction (16).

A voltage-sensitive influx of Ca²⁺ has been implicated in the regulation of cellular processes such as those occurring during cell growth, development, and differentiation (18–20). Enzymatic programs that regulate cell growth are activated by intracellular Ca²⁺ concentration in the micromolar range, which can be brought about by regional clustering of L-type Ca²⁺ channels, leading to high local concentrations of Ca²⁺ (19). Similarly, enhancements of voltage-dependent Ca²⁺ conductances could provide an additional mechanism by which extracellular growth signals are initiated via ras oncogene activation.

Ras activation of voltage-sensitive Ca²⁺ channels in differentiated neurons may be an initial step in the expression of Ras function. Several proto-oncogenes are expressed in post-mitotic cells (1); our results are consistent with their potential role in transmembrane signaling. An analogous role in a learning context may be played by the low molecular weight G protein, cp20, which increases after classical conditioning (21) and causes marked K⁺ current reductions quite similar to the reductions following Ras injection into type B cells in *Hermisenda* (11).

REFERENCES AND NOTES

- J. C. Lical and S. R. Tronick, in *The Oncogene Handbook*, E. P. Reddy and T. Curran, Eds. (Elsevier, New York, 1988); M. Barbacid, *Annu. Rev. Biochem.* **56**, 779 (1987); A. C. Dolphin, *Trends Neurosci.* **11**, 287 (1988); E. Santos and A. R. Nebreda, *FASEB J.* **3**, 2151 (1989).
- D. Bar-Sagi and J. R. Feramisco, *Science* **233**, 1061 (1986).
- J. D. Feramisco, M. Gross, T. Kamata, M. Rosenberg, R. W. Sweet, *Cell* **38**, 109 (1984); D. W. Stacey and H. F. Kung, *Nature* **310**, 508 (1984).
- N. Hagag, J. C. Lical, M. Graber, S. A. Aaronson, M. V. Viola, *Mol. Cell. Biol.* **7**, 1984 (1987).
- T. Alonso, R. O. Morgan, J. C. Marvizon, H. Zarbl, E. Santos, *Proc. Natl. Acad. Sci. U.S.A.* **85**, 4271 (1988); J. C. Lical, J. Moscat, S. A. Aaronson, *Nature* **330**, 269 (1987).
- L. S. Mulcahy, M. R. Smith, D. W. Stacey, *Nature* **313**, 241 (1985); M. R. Smith, S. J. DeGudicibus, D. W. Stacey, *ibid.* **320**, 540 (1986).
- A. Pandiella, L. Beguinot, L. M. Vicentini, J. Meldolesi, *Trends Pharmacol. Sci.* **10**, 411 (1989).
- J. M. Caffrey, A. M. Brown, M. D. Schneider, *Science* **236**, 570 (1987); C. F. Chen, M. J. Corbley, T. M. Roberts, P. Hess, *ibid.* **239**, 1024 (1988); M. Estacion, *J. Membrane Biol.* **113**, 169 (1990).
- M. R. Hanley, *Neuron* **1**, 175 (1988); J. I. Morgan and T. Curran, *Trends Neurosci.* **12**, 459 (1989).
- A. Yatani *et al.*, *Cell* **61**, 769 (1990).
- C. Collin *et al.*, *Biophys. J.* **58**, 785 (1990); D. L. Alkon and T. J. Nelson, *FASEB J.* **4**, 1567 (1990).
- L. K. Kaczmarek, *Adv. Second Messenger Phosphoprotein Res.* **22**, 113 (1989).
- F. McCormick, *Cell* **56**, 5 (1989).
- B. M. Willumsen, A. Christensen, N. L. Hubbert, A. G. Papageorge, D. R. Lowy, *Nature* **310**, 583 (1984); D. R. Lowy and B. M. Willumsen, *ibid.* **341**, 384 (1989).
- A. C. Dolphin, *Annu. Rev. Physiol.* **52**, 243 (1990); G. Schultz, W. Rosenthal, J. Hescheler, W. Trautwein, *ibid.*, p. 275.
- A. C. Lloyd, H. F. Paterson, J. D. H. Morris, A. Hall, C. J. Marshall, *EMBO J.* **8**, 1099 (1989).
- P. Hockberger, M. Toselli, D. Swandulla, H. D. Lux, *Nature* **338**, 340 (1989).
- H. A. Ives and T. O. Daniel, *Proc. Natl. Acad. Sci. U.S.A.* **84**, 1950 (1987).
- R. A. Silver, A. G. Lamb, S. R. Bolsover, *Nature* **343**, 751 (1990); M. Rogers and I. Hendry, *J. Neurosci. Res.* **26**, 447 (1990).
- A. S. Manalan and C. B. Klee, *Adv. Cyclic Nucleotide Protein Phosphorylation Res.* **18**, 227 (1984).
- T. J. Nelson, C. Collin, D. L. Alkon, *Science* **247**, 1479 (1990).
- The two-electrode voltage-clamp technique for *Hermisenda* neurons has been described (21, 23). After dissection, the *Hermisenda* pedal ganglion was treated with protease (2 mg/ml) (Sigma) for 30 min, and LP₁ was impaled with 2 to 2.5 megohm electrodes filled with 3 M CsCl₂ and then connected to a custom-made high-power voltage-clamp amplifier (Pelagic Electronics, Falmouth, MA). A third 1 megohm microelectrode was filled with Ras or control solutions, containing 5 mM tris, 2.5 mM MgCl₂, 0.5 mM EDTA, and 20 mM KCl; 1 M potassium acetate was used as charge carrier. The preparation was kept at 22°C and bathed in artificial sea-water solution containing 10 mM KCl, 50 mM MgCl₂, 10 mM BaCl₂, 327 mM tetramethylammo-
- nium (TEA), 10 mM tris (pH 7.4), 100 mM TEA, 3 mM 4-AP; osmolarity was 990 mosM. Pulse generation, data acquisition, and analysis was performed with pClamp (Axon Instruments, California). Immediately after impalement, a resting membrane potential of -45 to -55 mV was measured and then cells were voltage clamped at -60 mV. Current transients were low-pass filtered [corner frequency of 10 kHz, digitized at 200 μs per point and leak-corrected on line with a P/N protocol—a series of eight subpulses (P) of one-eighth the step amplitude (N)]. Inward currents, elicited with 150-ms, 10-mV depolarizing steps, were measured at a 30-ms time point before and every 10 min after iontophoretic injections (-10 nA for 10 min) of Ras or control solutions. H-Ras soluble proteins were purified from *Escherichia coli* (14). The prokaryotic vector (pJCL-30) places the murine *ras* genes under the control of the temperature-inducible λpL promoter. A 75% purity of the expressed proteins was first obtained on a Aca54 (molecular sizing) column, and 90% purity after a fast protein liquid chromatography (FPLC) mono Q column. After dialysis into 50% glycerol, proteins were stored at -20°C. Before use, proteins were solubilized in 10 mM tris (pH 8.0), 5 mM MgCl₂, and 1 mM EDTA.
- C. Collin, H. Ikeno, J. F. Harrigan, I. Lederhendler, D. L. Alkon, *Biophys. J.* **54**, 955 (1988).
- We thank C. Braham, R. Etcheberrigaray, F. Gusovsky, D. Lester, T. J. Nelson, and J. L. Olds for their helpful comments.

8 June 1990; accepted 24 September 1990

Hot Spots for Growth Hormone Gene Deletions in Homologous Regions Outside of Alu Repeats

CINDY L. VNEŇAK-JONES AND JOHN A. PHILLIPS III

Familial growth hormone deficiency type 1A is an autosomal recessive disease caused by deletion of both growth hormone-1 (GH1) alleles. Ten patients from heterogeneous geographic origins showed differences in restriction fragment length polymorphism haplotypes in nondeleted regions that flanked GH1, suggesting that these deletions arose from independent unequal recombination events. Deoxyribonucleic acid (DNA) samples from nine of ten patients showed that crossovers occurred within 99% homologous, 594-base pair (bp) segments that flanked GH1. A DNA sample from one patient indicated that the crossover occurred within 454-bp segments that flanked GH1 and contained 274-bp repeats that are 98% homologous. Although Alu repeats, which are frequent sites of recombination, are adjacent to GH1, they were not involved in any of the recombination events studied. These results suggest that length and degree of DNA sequence homology are important in defining recombination sites that resulted in GH1 deletions.

INDIVIDUALS WITH FAMILIAL ISOLATED growth hormone deficiency (IGHD) type 1A have a complete absence of growth hormone (GH) and frequently develop immune intolerance to exogenous GH (1–3). The molecular basis of this autosomal recessive disorder is the deletion of both GH1 alleles. Although the incidence of IGH1 type 1A is unknown, ~35 unrelated cases from 15 countries have been reported.

Differences in geographic origin of patients and the heterogeneity seen in restriction fragment length polymorphism (RFLP) haplotypes in nondeleted sequences that flank GH1 suggest that these deletions represent independent recombinational events.

The GH1 locus has been mapped by *in situ* hybridization to chromosome 17q22–24 and is normally present at the 5' end of the 66.5-kb human GH gene cluster. The GH gene cluster includes (5' to 3') GH1, chorionic somatomammotropin pseudogene-1 (CSHP1), chorionic somatomammotropin-1 (CSH1), growth hormone-2 (GH2), and chorionic somatomammotropin-2 (CSH2), as well as 48 Alu repeats (4,

C. L. Vnencak-Jones, Departments of Pathology and Pediatrics, Vanderbilt University School of Medicine, Nashville, TN 37232.
J. A. Phillips III, Departments of Pediatrics and Biochemistry, Vanderbilt University School of Medicine, Nashville, TN 37232.